Selective post-column liquid chromatographic determination of sugars in spent sulphite liquor with two enzymatic electrochemical detectors in parallel

G. MARKO-VARGA*

Department of Analytical Chemistry, University of Lund, P.O. Box 124, S-221 00 Lund (Sweden)

E. DOMINGUEZ

Department of Pharmacy, Food Analysis and Nutrition, University of Alcalá de Henares, Madrid (Spain)

B. HAHN-HÄGERDAL

Department of Applied Microbiology, University of Lund, P.O. Box 124, S-221 00 Lund (Sweden)

and

L. GORTON

Department of Analytical Chemistry, University of Lund, P.O. Box 124, S-221 00 Lund (Sweden)

SUMMARY

   Matrix components in spent sulphite liquor interfere with the liquid chromatographic determination of sugars. High selectivity can be obtained by coupling the column with two immobilized enzyme reactors and amperometric detection. The carbohydrates eluted from the column are mixed with a make-up flow, consisting of a nicotinamide adenine dinucleotide (NAD^+) buffer. Because the chromatographic separation of sugars in spent sulphite liquor is incomplete, the column effluent is split into two detection paths, each containing an immobilized enzyme reactor, with different selectivity, coupled on-line with amperometric flow-through cells. One reactor contains mutarotase, glucose dehydrogenase and galactose dehydrogenase and the other also contains an additional enzyme, xylose isomerase. The carbohydrates are oxidized to form an equivalent amount of reduced coenzyme (NADH), which is detected electrochemically with an electrode modified by a phenoxazine derivative.

INTRODUCTION

   In recent years there has been great interest in fermenting cheap sources of carbohydrates to ethanol. Carbohydrate mixtures derived from lignocellulosic materials are such sources[1]. They can be produced by either acid or enzymatic hydrolysis, usually preceded by heat treatment. Sulphite pulping of lignocellulose also gives a fermentable by-product, known as spent sulphite liquor. Typically, a lignocellulose hydrolysate may contain a mixture of D-glucose, D-mannose, D-galactose, L-arabinose and D-xylose[2]. In addition, when a lignocellulose hydrolysate is obtained

by enzymatic hydrolysis, it will also contain D-cellobiose[3]. The pretreament and hydrolysis processes create compounds such as acetic acid and furfural, which are inhibitory to the microorganisms fermenting the carbohydrates to ethanol. In this context, fermentation with a combination of ordinary baker's yeast, *Saccharomyces cereviseae*, and the enzyme xylose isomerase (glucose isomerase) has been found to be superior to fermentation with other yeasts[4,5]. D-Xylose is not fermentable unless isomerized to D-xylulose[3]. To follow the process there is a need for an analytical procedure that permits the quantification of the saccharides in the fermentor, including D-xylulose, during fermentation. In this investigation we used spent sulphite liquor, supplemented with D-xylulose and D-cellobiose, as a model fermentation substrate.

We have previously described detection systems for flow-injection analysis (FIA) and liquid chromatography (LC) for the selective determination of D-xylose and D-xylulose[6,7]. The detection system is based on post-column immobilized enzyme reactors (IMER), which oxidize the sugars selectively to form dihydronicotinamide adenine dinucleotide, (NADH), followed by selective electrochemical detection of NADH at a chemically modified electrode (CME)[6,7]. There has recently been great interest in utilizing CMEs as electrochemical detectors in analytical flow systems because of their unique property of enhancing sensitivity and selectivity[8,9]. By a combination of two selective steps in the detection system, the enzymatic (IMER) and the electrochemical (CME), further selectivity can be gained, which is important in the analysis of complex samples.

This paper extends previous systems by including two post-column enzyme electrochemical detection systems working in parallel for the selective monitoring of the concentrations of sugars in spent sulphite liquor.

Owing to the difficulty of achieving the complete chromatographic separation of all monosaccharides, the effluent from the column is split into two streams of equal flow-rates, each passing through a post-column enzyme electrochemical detection system but with different selectivities. In one detection path three enzymes are immobilized: mutarotase, galactose dehydrogenase, and glucose dehydrogenase. In this reactor all saccharides, except D-xylulose, are oxidized to form NADH. In the other path, a reactor containing an additional enzyme, xylose isomerase, is co-immobilized with the other three enzymes. Thus, D-xylulose is also oxidized to form NADH in this reactor. The NADH formed in both reactors is further transported to electrochemical flow-through cells where it is selectively and catalytically oxidized at 0 mV *vs.* SCE at an electrode chemically modified with a phenoxazine derivative[6,7,10,11].

EXPERIMENTAL

Flow system

The basic components of the flow system consisted of an LC pump, Model 2150 (LKB, Bromma, Sweden), an injector, Model 7045 (Rheodyne, Cotati, CA, U.S.A.), with sample loops of 5, 10, 20, 50, 100 and 200 μl and separation columns of the Aminex HPX 87 type (300 × 7.8 mm I.D.), containing sulphonic groups.

Three commercially available columns were used, Aminex HPX 87P (Pb^{2+} loaded), Aminex HPX 87C (Ca^{2+} loaded) and Aminex HPX 87H (H$^+$ form), all

supplied by Bio-Rad Labs., Richmond, CA, U.S.A. The HPX-87H column was used at 40°C with 5 mM sulphuric acid as the mobile phase. A K$^+$ ligand-exchange column was prepared by treating an Aminex HPX 87H column with 0.1 M K$_2$HPO$_4$ (pH 7.0) for 24 h to load the sulphonate sites with K$^+$, and used with the same solution as the mobile phase. Li$^+$ and Mg^{2+} columns were made by treating Aminex HPX 87P columns with stock metal ion solution prepared by dissolving analytical-reagent grade metal nitrate in water to make 0.1 M solutions. The pH was adjusted to 6.5 and the solution was allowed to pass through the column for 24 h to load the polymer resin. After loading, the resin was removed from each column and dissolved in 1 M nitric acid and analysed with atomic absorption spectrometry to ensure that no traces of Pb^{2+} remained. Subsequently the columns were equilibrated with water before use. The HPX-87P and HPX-87C columns were used as received.

The mobile phase was carefully deaerated. It consisted of water in all instances, except for the H$^+$ and the K$^+$-loaded columns (see above). The mobile phase was prethermostated to 40°C for the column in the protonated form and otherwise to 85°C by passing the carrier through a 2-ml loop in the column oven, Model 2155 (LKB), prior to injection of sample[12]. Prethermostating the mobile phase promotes separation of the saccharides.

Spent sulphite liquor was prepared as follows before samples were injected into the LC system. The liquid was neutralized by the addition of sodium hydroxide to a final pH of 7.0, filtered through 0.40-μm membrane filters (Millex-HV; Millipore, Milford, MA, U.S.A.) to remove solid particles, and then passed through a solid-phase extraction column for sample clean-up[12,13]. The extraction column was conditioned by passivation prior to sample passage, as described previously[14]. A strong anion-exchange phase was used, containing quaternary amine functional groups (SAX, volume 3 ml; Analytichem International, kindly donated by Mr. G. Oresten, Sorbent, Västra Frölunda, Sweden). The sample solution was further diluted with water before injection (see Results and Discussion). A small guard column was used when pretreated and diluted samples of spent sulphite liquor were introduced into the chromatographic system. This consisted of a stainless-steel column (2.5 cm × 0.4 cm I.D.), filled with the same material as the Aminex HPX-87P column.

The effluent from the column was mixed with a deaerated make-up flow consisting of 0.7 M phosphate buffer (pH 7.0) containing 21 mM magnesium nitrate, 7 mM EDTA and 14 mM nicotinamide adenine dinucleotide (NAD$^+$), necessary for the enzymatic reaction (see below). The EDTA was added to the make-up flow to complex metal ions leaking from the column that would otherwise poison the enzymes[12]. However, EDTA alone may inactivate the enzymes, but this is counteracted by the addition of Mg^{2+} to the buffer[12]. The make-up flow was delivered by a second LC pump, Model 2150 (LKB), passing through a pulse damper (Touzart Matignon, Paris, France). The combined flows passed through a 50-μl single bead string reactor (SBSR) (100 mm × 0.8 mm I.D.), filled with solid glass beads, diameter 0.5 mm, to promote complete mixing and counteract band-broadening effects[12,13].

The three-electrode amperometric flow-through cell was of the confined wall-jet type, and has been described previously[15]. The working electrode consisted of a polished and pretreated graphite rod[13], RW 001 (Ringsdorff Werke, F.R.G.), the 0.0731-cm^2 flat surface of which was exposed to the flow. The surface of the graphite was chemically modified by introduction of a mediator to promote electrocatalytic

oxidation of NADH. This was achieved by applying a few droplets of a dissolved redox mediator (a bisphenoxazinyl derivative of terephthalic acid[11]) in acetone and allowing the solvent to evaporate. The modifier contains an extended aromatic ring system and is strongly adsorbed on the surface of the electrode. The surface coverage of the mediator was at least $2 \cdot 10^{-9}$ mol cm^{-2} (ref. 11), determined by cyclic voltammetry, before insertion of the electrode in the flow cell. Fig. 1 shows the cyclic voltammo-grams obtained for (a) a naked and (b) a chemically modified graphite electrode. The surface coverage of the adsorbed mediator can be evaluated by integration of the area under the waves. The formal potential of the adsorbed mediator is given by taking the mean potential of the peaks of the oxidation and reduction waves. Fig. 1c shows evidence of the electrocatalytic properties of the adsorbed mediator in the presence of NADH. Fig. 1 reveals that the catalytic reaction between NADH and the adsorbed
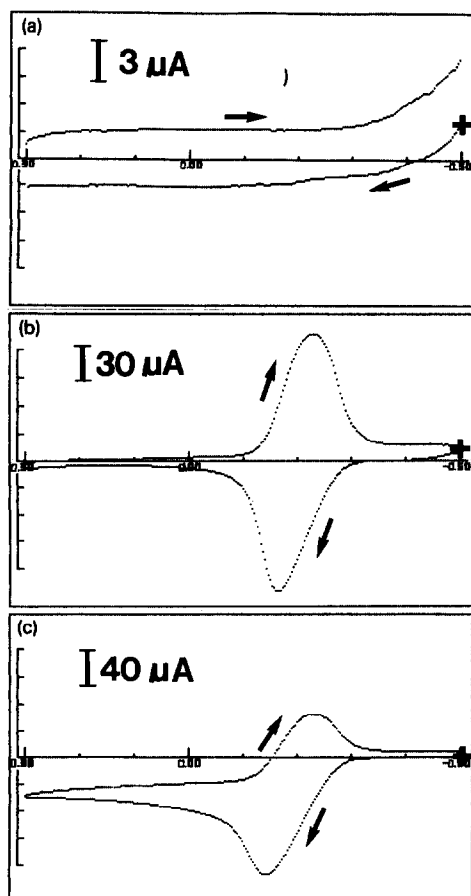

Fig. 1. Cyclic voltammograms of (a) a naked graphite electrode, (b) graphite chemically modified with a bisphenoxazinyl derivative of terephthalic acid, (c) as (b) but in the presence of 8 mM NADH. The contacting electrolyte was 0.25 M phosphate buffer (pH 7.0). Surface coverage, 7.5 nmol cm^{-2}; sweep rate, 100 mV s^{-1}. +, Starting potential. The x-axis denotes the applied potential $vs.$ a saturated calomel reference electrode.

mediator is fast and also that the catalytic reaction can occur at potentials substantially lower than 0 mV, as the anodic peak potentials of the cyclic voltammograms in Fig. 1b and c, with and without the presence of NADH, are almost identical[10].

A platinum-wire counter electrode and an Ag/AgCl (0.1 M KCl) reference electrode were used. The cell was connected to a potentiostat (Zäta Elektronik, Lund, Sweden). The applied voltage was 0 mV vs. Ag/AgCl throughout all the experiments[11,13].

In the final flow system (Fig. 2), two identical electrochemical cells were used, each connected to one potentiostat. To split the combined flows after mixing with the make-up flow, a gradient mixer (GM), Model 2152 (LKB), was used in the backward mode and at the highest frequency to yield an optimum splitting ratio and to prevent band broadening.

In some experiments a spectrophotometric flow-through detector, Model 2151 (LKB), was used at 340 nm to determine the NADH formed in the flow system.

Enzyme reactors

The following enzyme preparations were used. Xylose isomerase (XI) (E.C. 5.3.1.5) from *Streptomyces* sp. was generously supplied by Miles Kali Chemie (Hannover, F.R.G.) as a suspension with an activity of 4.5 U mg^{-1} protein. Mutarotase (MT) (E.C. 5.1.3.3) from porcine kidney was purchased from Sigma (St. Louis, MO, U.S.A.), cat. no. M-4007, dissolved in 3.2 M ammonium sulphate, with an activity of 5800 U mg^{-1} protein. Glucose dehydrogenase (GDH) (E.C. 1.1.1.47) from *Bacillus megaterium* was purchased from Merck (Darmstadt, F.R.G.), cat. no. 13732,
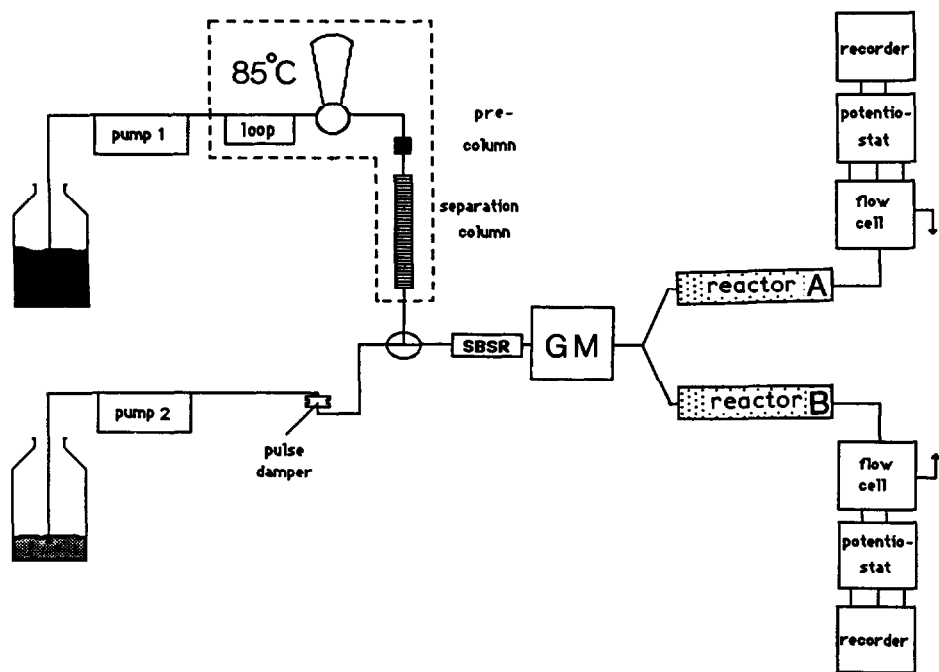

Fig. 2. Final chromatographic set-up. For details, see text.

as a lyophilized powder with an activity of 220 U mg^{-1} protein. Based on experience, it was used as received without further treatment[6,13]. Galactose dehydrogenase (GaDH) (E.C. 1.1.1.48) from recombinant *Escherichia coli* using *Pseudomonas fluorescens* gene, from Sigma, cat. no. G-6637, obtained as a suspension in 3.2 *M* ammonium sulphate with an activity of 50 U mg^{-1} protein, was kindly donated by Mr. H. Toomson (Kebo Lab, Stockholm, Sweden).

Prior to immobilization, XI, MT and GaDH were dialysed against a large excess of 0.1 *M* phosphate buffer (pH 7.0) to remove the ammonia and other low-molecular-weight substances that could otherwise interfere in the immobilization reaction. The units given for XI are as described previously[6], and those for MT, GDH and GaDH are according to the manufacturers' specifications.

Controlled-pore glass (CPG-10) from Serva, pore diameter 47 nm and particle size 37–74 μm, was washed, dried, silanized with 3-aminopropyltriethoxysilane and activated with glutaraldehyde according to previously published procedures[16,17] before coupling of the enzymes. The Zr–silica was a zirconium-covered silica phase, LiChrospher Si-500, consisting of 10-μm spherical silica with a pore size of 500 Å, kindly donated by Mr. Gyula Szabo (Bioseparation Technologies, Budapest, Hungary). It was silanized and activated with glutaraldehyde according to the procedure outlined above for the CPG.

Enzyme reactor I. To 1 g of the activated CPG-10 support, an enzyme mixture of 746 U of XI, 17 400 U of MT, 10 000 U of GDH and 375 U of GaDH dissolved in 0.1 *M* phosphate buffer (pH 7.0) was added. After reducing the air pressure of the reaction mixture, the coupling was allowed to proceed overnight at 4°C. The coupling yield was determined by analysis, measuring the reaction rate of the remaining unimmobilized enzyme in the buffer solution. It was found to be 43% for XI using 500 m*M* D-fructose and 7.5 m*M* NAD$^+$, 59% for GDH using 250 m*M* D-glucose and 2.5 m*M* NAD$^+$ and 60% for GaDH using 250 m*M* D-galactose and 2.5 m*M* NAD$^+$. The zero-order reaction conditions for evaluation were made at 25°C and in 0.1 *M* phosphate buffer (pH 7.0) containing 8 m*M* magnesium nitrate. The NADH produced was measured spectrophotometrically at 340 nm. The coupling yield for MT was not specifically evaluated[6,13]. The enzyme–CPG was packed into a reactor having a low dead volume[6]. Throughout, a volume of 250 μl was used for this reactor.

Enzyme reactor II (denoted A in Fig. 2). To 1 g of the activated Zr–silica an enzyme mixture of 746 U of XI, 17 400 U of MT, 10 000 U of GDH and 375 U of GaDH was added.

Enzyme reactor III (denoted B in Fig. 2). To 1 g of the activated Zr–silica an enzyme mixture of 17 400 U of MT, 10 000 U of GDH and 375 U of GaDH was added. Reactors II and III were both slurry packed into 79-μl stainless-steel reactors to obtain optimum packing of the enzyme–glass using a highly viscous, 5.0 *M* sucrose slurry and a high-pressure pump between 0.28 and 1.12 kg m^{-2}. When not in use, all reactors were filled with 0.1 *M* phosphate buffer containing 1 *M* sodium chloride for stabilization of the enzymes[12,13].

Chemicals

NAD$^+$ and NADH were obtained from Merck (cat. no. 24542) and from Sigma (cat. no. N-8129), respectively. The sugars L-arabinose, D-xylose, D-glucose, D-cellobiose, D-galactose and D-mannose were obtained from Sigma and D-xylulose was

produced and purified in this laboratory[7]. The water used throughout was of the highest purity grade, Milli-RQ4 (Millipore).

RESULTS AND DISCUSSION

Post-column LC detection scheme

In the presence of NAD$^+$, GDH catalyses the oxidation of the β-anomeric form of a series of aldoses whereby a lactone and NADH are produced. The reaction is exemplified below with the oxidation reaction of β-D-glucose:

$$\beta\text{-D-glucose} + \text{NAD}^+ \overset{\text{GDH}}{\rightleftharpoons} \delta\text{-gluconolactone} + \text{NADH} \tag{1}$$
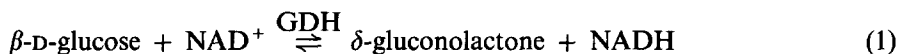
Other carbohydrates that are oxidized according to a similar reaction scheme are D-xylose, D-mannose, D-cellobiose, D-lactose, D-ribose, D-deoxyglucose and D-glucosamine[12,15].

Similarly to GDH, GaDH catalyses the oxidation of the β-form of a series of carbohydrates. The best known are D-galactose and L-arabinose[18]:

$$\beta\text{-D-galactose} + \text{NAD}^+ \overset{\text{GaDH}}{\rightleftharpoons} \gamma\text{-galactonolactone} + \text{NADH} \tag{2}$$
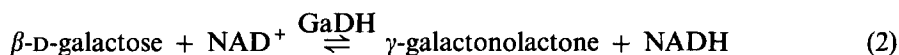
The reversibility of reactions 1 and 2 is counteracted by the irreversible addition of water to the lactone formed[19]:

$$\text{lactone} + \text{H}_2\text{O} \longrightarrow \text{D-acid} \tag{3}$$

The rate with which this addition occurs is pH dependent and is governed by a more alkaline pH, especially for the lactones produced in reaction 2[20].

The sum of the reactions is thus an irreversible oxidation of the β-form of the sugars:

$$\beta\text{-form} + \text{NAD}^+ + \text{H}_2\text{O} \xrightarrow{\text{dehydrogenase}} \text{D-acid} + \text{NADH} \tag{4}$$
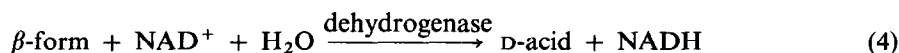
constituting the thermodynamic driving force for the production of the NADH for which the detection system is designed (see below).

At mutarotational equilibrium, a substantial amount of each of the above-mentioned saccharides occurs in the corresponding α-anomeric form, which is not oxidizable by the dehydrogenases. To make this portion of the carbohydrates detectable and to make the detection system independent of whether mutarotational equilibrium is at hand, MT is co-immobilized with the dehydrogenases. MT catalyses the interconversion between the two anomeric forms:

$$\alpha\text{-D-form} \overset{\text{MT}}{\rightleftharpoons} \beta\text{-D-form} \tag{5}$$

thus making the entire concentration of the saccharide detectable.

D-Xylulose is a ketose for which no commercial dehydrogenase is available for efficient oxidation and NADH production. However, D-xylulose can be isomerized to form α-D-xylose with XI:

$$\text{D-xylulose} \overset{\text{XI}}{\rightleftharpoons} \alpha\text{-D-xylose} \qquad (6)$$

This enzyme is best known as glucose isomerase and is commercially used for the isomerization of D-glucose to D-fructose[21,22]. The anomeric form of the ketose taking part in reaction 6 is not fully known[23-25]. Subsequent mutarotation of the α-D-xylose (reaction 5), and oxidation of the β-form (reaction 3), make D-xylulose detectable.

The NADH formed in the reactors is transported with the flow carrier to the electrochemical flow-through cell where it is electrochemically oxidized[10]. Through surface modification of the graphite electrode with an electrocatalytically active aromatic redox mediator (a bisphenoxazinyl derivative of terephthalic acid[11]), the NADH can be selectively and rapidly oxidized at 0 mV *vs.* Ag/AgCl[11,13]. The net reaction is

$$\text{NADH} \xrightarrow{E_{\text{appl}} > E^{0\prime}_{\text{mediator}}} \text{NAD}^+ + \text{H}^+ + 2\text{e}^- \qquad (7)$$
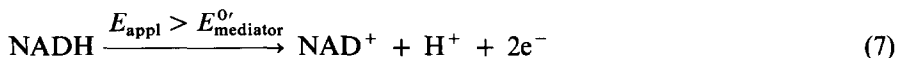
where E_{appl} denotes the applied potential of the modified graphite electrode and $E^{0\prime}_{\text{mediator}}$ denotes the formal potential of the adsorbed mediator.

The modification of the electrode surface decreases the large overvoltage (*ca.* 1 V) and circumvents electrode fouling, which are serious drawbacks with the direct electrochemical oxidation of NADH[26,27]. Most common low-molecular-weight interferents are neither oxidized nor reduced at the applied potential[15,28]. The background current and noise levels of the graphite electrode material are also at their lowest values around 0 mV[13]. Overall, this makes the detection mode close to the optimum for the determination of NADH.

There are several aspects to be considered when making use of a sequence of enzymatic reactions in a detection system[29]. By co-immobilizing the enzyme on the same support or in the same matrix, the reaction sites become closer and the kinetics of the reactions, converting intermediates and driving unfavourable equilibria to the product side, become more favourable than if immobilized one at a time with subsequent mixing of the different enzyme–glass portions[29,30]. The kinetics and equilibrium of each of the different enzymatic steps in the sequence should not counteract each other and the $K_{\text{ps}}^{\text{app}}$ ($= V_{\text{max}}/K_{\text{M}}^{\text{app}}$)[17] of the following enzyme in a sequence must be greater than the preceding enzyme activity[29].

The optimum ratio of the enzymes can be calculated on the basis of the properties of each individually immobilized enzyme. The ratio obtained when co-immobilized cannot be predicted as the kinetics, denaturation effects and overall yield of the binding reactions to the support cannot be predicted from a mixture of several enzymes. A detailed study of the optimum ratio when co-immobilizing XI, MT and GDH was made separately[31], the influence of the thermodynamic driving force to form NADH (reaction 4) and the overall enzyme kinetics were considered. The

properties of immobilized GaDH were studied separately[32]. Experiments from these studies were guidelines for the enzymatic ratios used in the IMERs in this study.

Post-column parameters

pH dependence. Previous papers on reactors containing co-immobilized XI, MT and GDH have been used as parts of the detection system in both FIA[6,31] and LC applications[7]. As an extension to our previous work, a fourth enzyme, GaDH, was co-immobilized with the other three to increase the number of detectable sugars.

To minimize band-broadening effects of the chromatographic peaks in the IMER, the volume of the reactor is necessarily small. This may result in the conversion efficiencies of some substrates being low, owing to the restricted amount(s) of immobilized enzyme(s) that can be contained within the reactor. It is therefore necessary to optimize the detection system so that the enzymes can be utilized in such a way that the highest and long-term stable response conditions prevail.

Reactor I was investigated in the FIA mode by omitting the separation column and the gradient mixer (see Fig. 2) for evaluation of the pH optimum for detection of the sugars. The substrates were injected one at a time in these experiments. Reactions 1–7 all have different pH optima. The combined effects of these reactions on the detection system are depicted in Fig. 3. The reaction rate between NADH and the adsorbed mediator on the graphite surface is governed by a more acidic pH[10], which is reflected in curve b.

It was concluded from previous investigations that immobilized GDH has a broad optimum pH range[13,15]. The responses to equal concentrations of NADH and D-glucose are almost identical at pH 6–7. At more alkaline pH, the response to D-glucose is lower than that to NADH, reflecting a decrease in the turnover rate of GDH. The addition of water to the lactone, formed in reaction 1, is governed by higher pH values which could otherwise be expected to increase the overall reaction rate (reaction 4) for NADH formation[20]. The activity of GDH differs for the various substrates. D-Glucose (Fig. 3a) is much more efficiently oxidized than, *e.g.*, D-xylose (Fig. 3e). The effect of the addition of water to the lactone is greater for the oxidation of
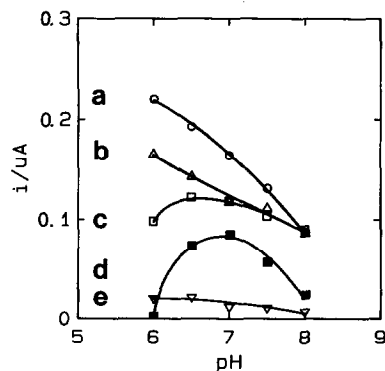

Fig. 3. Response *vs.* pH for 20 μl of (a) 0.5 mM D-glucose, (b) 0.35 mM NADH, (c) 0.5 mM D-galactose, (d) 9.0 mM D-xylulose and (e) 0.15 mM D-xylose with reactor I. The flow system was operated in the FIA mode, using 0.1 M phosphate buffer (pH 7.0) as the eluent (0.75 ml min^{-1}); applied potential, 0 mV *vs.* Ag/AgCl. For details, see text.
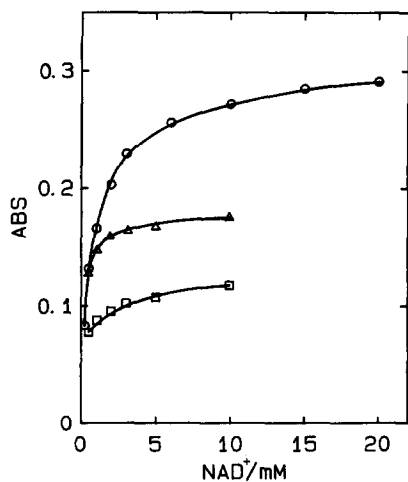
Fig. 4. Influence of the concentration of NAD^+ in the carrier flow in a flow-injection manifold on the response for (○) D-galactose (0.4 mM); (△) D-xylose (1 mM) and (□) D-xylulose (1 mM). The flow-rate through reactor I was for (○) 1.0 and for (△) and (□) 0.6 ml min^{-1}. Injection volume, 50 μl.

D-galactose (Fig. 3c), where proportionally higher response values are obtained at higher pH. The optimum response for D-xylulose is found close to pH 7, mainly reflecting the optimum activity for immobilized XI found at pH 7[6].

The combined effects of pH on the electrocatalytic response factor, on the addition of water to the lactones and on the activities of the four co-immobilized enzymes indicate that pH 7 should be the optimum for detection, especially for the substrates with low turnover rates in the reactor, namely D-xylose and D-xylulose. This pH was therefore used throughout all the experiments described below.

NAD$^+$ dependence. The dependence of the concentration of NAD^+ in the make-up flow was also investigated with the equipment used in the FIA mode and with a spectrophotometric flow-through detector, at 340 nm, for evaluation of the NADH formed. Fig. 4 shows the effect on the response for three sugars, D-galactose, D-xylose and D-xylulose, when increasing the NAD^+ concentration in the make-up flow from 0.5 to 10 mM or more. The direct influence of the NAD^+ concentration on reactions 1 and 2 is clearly depicted, in addition to the indirect influence on reactions 5 and 6 to increase the driving force for NADH production. It is also known from earlier experiments[6] that a high concentration of NAD^+ governs the driving force for D-xylulose oxidation (reactions 5 and 6), as stated above. At a higher concentration than about 10 mM the response levels off to a constant value. Owing to the high cost of NAD^+, a final concentration of 14 mM NAD^+ in the make-up flow was chosen, resulting in an NAD^+ concentration of 2 mM in the IMER. Response efficiencies between 72 and 90% of the maximum values at 10 mM NAD^+ in the IMER were obtained with this NAD^+ concentration for the sugars depicted in Fig. 4: D-galactose 72%, D-xylose 88% and D-xylulose 90%. These values are high enough to obtain high detection responses.

Chromatographic separation

Sugars can be separated with varying success on polymer-based ion-exchange or ligand-exchange columns. The separation is largely dependent on the cation (proton or metal ion) bound to the stationary phase and the type of sugar interacting with it[33-35]. The polymeric columns loaded with metal ions show good stabilities. Minor metal leakage may, however, occur from the resin[36] and may interact in a negative way when post-column immobilized enzyme reactors are used[12]. The decline in performance with these columns is almost always due to the introduction of contaminants present in the sample or in the mobile phase that precipitate or clog the column. This can be overcome or at least greatly decreased by using proper sample clean-up procedures. The sugar molecules are uncomplexed in the aqueous mobile phase but are bound to the stationary phase as complexes with the metal ion. It is essential here that an aqueous mobile phase is used that is compatible with the enzyme electrochemical detection system. The dominating mechanism for separation of the sugars is mainly related to the stability constants, K_{stab}, of the complexes formed. The capacity factor, k', can be expressed as[35]

$$k' = V_s/V_m \, [M^{x+} \, (aq.)] \, K_{stab} \tag{8}$$

where V_s is the volume of the stationary phase, V_m is the volume of the mobile phase and $x+$ is the valency of the metal ion, M.

Five different metal-loaded columns and a column in the H^+ form were studied for their abilities to separate the sugars most commonly present in lignocellulose hydrolysates, *viz.*, D-glucose, D-mannose, D-galactose, L-arabinose and D-xylose. D-Xylulose and D-cellobiose were added to the mixture for reasons indicated in the Introduction. All columns used were of equal size and equal cross-linking for otherwise identical conditions when evaluating the binding interaction. Three commercially available columns were used (H^+, Ca^{2+} and Pb^{2+}) and the other three (K^+, Li^+ and Mg^{2+}) were prepared according to the scheme outlined under Experimental.

TABLE I

CHROMATOGRAPHIC CHARACTERISTICS OBTAINED WITH THE SIX INVESTIGATED LIGAND-EXCHANGE COLUMNS USING THE ENZYMATIC ELECTROCHEMICAL DETECTOR

Ce = D-Cellobiose, Glu = D-glucose, Xo = D-xylose, Gal = D-galactose, Ara = L-arabinose, Xy = D-xylulose, Man = D-mannose.

Ligand	Retention time (min)						
	Ce	Glu	Xo	Gal	Ara	Xy	Man
H^+	7.0	8.4	9.0	9.2	9.8	9.6	8.2
K^+	7.8	10.2	10.7	10.9	11.2	10.7	10.9
Li^+	7.6	9.2	10.3	10.4	11.8	12.0	10.8
Mg^{2+}	7.0	9.0	9.8	9.0	11.2	11.1	10.0
Ca^{2+}	8.0	10.0	10.8	11.3	13.3	13.6	11.6
Pb^{2+}	10.7	12.6	13.6	13.3	15.4	16.4	16.6

Single-line detection system

The influences of the different metal ions on the separation of the sugars present in spent sulphite liquor are shown in Table I and in Fig. 5, where the k' values are
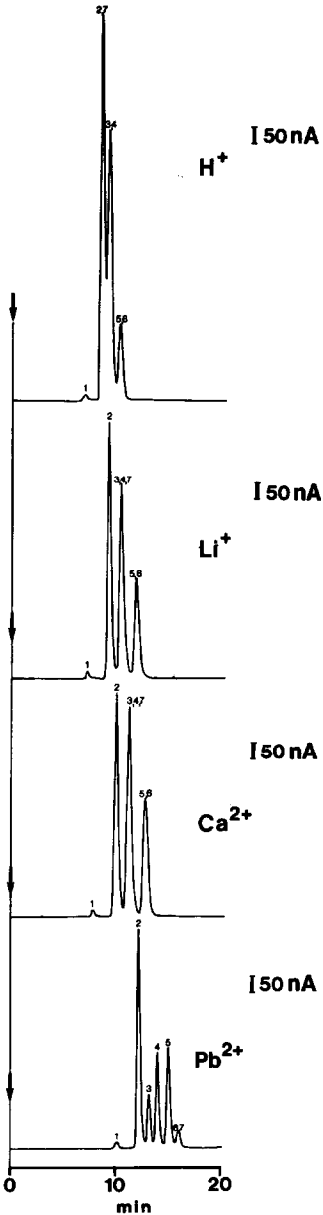

Fig. 5. Chromatograms obtained with different columns for 10 μl of spent sulphite liquor, diluted 30-fold and spiked with D-cellobiose and D-xylulose. Column flow-rate, 0.6 ml min^{-1}; make-up, 0.1 ml min^{-1}. Concentrations of sugars: 1.5 mM D-cellobiose (peak 1), 0.7 mM D-glucose (peak 2), 1.4 mM D-xylose (peak 3), 0.4 mM D-galactose (peak 4), 0.4 mM L-arabinose (peak 5), 1.5 mM D-mannose (peak 6) and 3.6 mM D-xylulose (peak 7).

shown to increase as the stabilities of the complexes increase. Fig. 5 shows the retention patterns for some of the different columns, with increasing binding strength. Pb^{2+} has the best binding capacity for the sugar mixture. Ca^{2+}, Li^+ and Mg^{2+} have similar strengths. However, the order of retention differs for the different columns (Table I). The H^+ and K^+ columns are similar in separation capacity, having the weakest complex binders of the six types studied. The Pb^{2+} column resolves all sugars except D-mannose and D-xylulose, which elute in the same peak (6, 7 in Fig. 5). The peak is broad not only because of band broadening but also because the retention times differ but not sufficiently to result in complete separation.

The dependence of the injection volume on the resolution of these two sugars was therefore investigated to see whether a smaller injection volume could increase the resolution sufficiently to separate the two sugars. No separation between D-mannose and D-xylulose was achieved at any injection volume (data not shown). However, it can be seen from Table II, illustrating the response and band broadening at the peak half-height, $w_{\frac{1}{2}}$, that by using injection volumes larger than 100 μl a much higher response will not be obtained but rather a larger dispersion, which leads to a decrease in resolution. The choice of the injection volume will also be dependent on the concentration of the sugars in the sample. For spent sulphite liquor, a sample loop of 10 μl was chosen because it resulted in a good resolution and no substantial decrease in signal response was found compared with a 20-μl loop.

The flow-rate of the make-up and the injection volume may contribute substantially to the band broadening[37]. It was therefore investigated whether optimizing these parameters could increase the resolution of D-mannose and D-xylulose and make their quantification possible. Fig. 6 shows the effect on the response of the flow-rate of the make-up. The optimum flow-rate yielding the highest response values was *ca.* 0.1 ml min^{-1}. In these experiments the composition of the make-up was kept constant. At lower make-up flow-rates, the sugars will be less diluted and the residence time in the IMER will be longer. These two effects will

TABLE II

INFLUENCE OF THE INJECTION VOLUME (5–200 μl) ON THE PEAK HEIGHT, AND BAND BROADENING, $w_{\frac{1}{2}}$, IN THE CHROMATOGRAMS OF 1.3 mM D-XYLOSE, 0.8 mM D-GLUCOSE, 0.5 mM D-GALACTOSE, 0.45 mM L-ARABINOSE, 30 mM D-XYLULOSE AND 2.2 mM D-CELLO-BIOSE WITH REACTOR I

Flow-rate, 0.6 ml min^{-1}; make-up flow, 0.1 ml min^{-1}.

| Sugar	Peak height, i (nA)					Peak broadening, $w_{\frac{1}{2}}$ (min)				
	Injection volume					Injection volume				
	5 μl	10 μl	50 μl	100 μl	200 μl	5 μl	10 μl	50 μl	100 μl	200 μl
D-Cellobiose	8	13	55	62	78	0.36	0.40	0.43	0.49	0.63
D-Glucose	310	505	1330	2425	3747	0.38	0.41	0.44	0.46	0.53
D-Xylose	70	105	300	550	850	0.38	0.41	0.44	0.49	0.62
D-Galactose	125	200	355	488	575	0.45	0.47	0.49	0.59	0.92
L-Arabinose	130	210	360	490	525	0.44	0.48	0.55	0.63	0.78
D-Xylulose	20	28	85	138	225	0.56	0.61	0.66	0.71	0.84
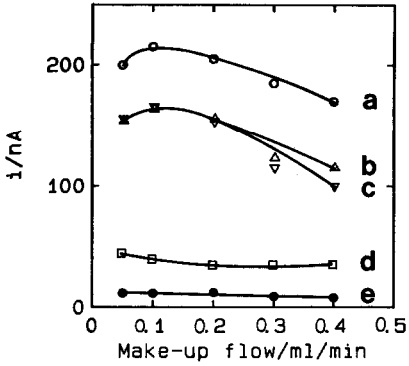
Fig. 6. Influence on the response of the make-up flow for (a) 0.7 mM D-glucose, (b) 0.7 mM D-galactose, (c) 0.73 mM L-arabinose, (d) 2.0 mM D-xylose and (e) 1.2 mM D-xylulose. Injection volume, 10 μl; flow-rate, 0.6 ml min^{-1}.

enhance the concentration of NADH especially for the sugars that do not yield 100% conversion efficiencies to form NADH. The response of the electrochemical detector is, however, governed by a higher flow-rate. The combined effects of higher NADH concentrations at a lower flow-rate of the make-up and a higher response of the CME at a higher flow-rate of the make-up are depicted in Fig. 6. For sugars with high conversion efficiencies an increase in the flow-rate from 0.05 to 0.1 ml min^{-1} will result in an increased response owing to a more efficient mass transport of NADH to the electrode surface. A further increase in flow-rate will only increase the band broadening of the peak and hence lower the response. For sugars with low conversion efficiencies an increase in the flow-rate from 0.05 to 0.1 ml min^{-1} will result in a decreased response owing to a lower residence time in the IMER and hence in a lower NADH production. An optimum flow-rate of the make-up was therefore concluded to be *ca.* 0.1 ml min^{-1} and was used for all subsequent experiments. Table III shows the response factors for the seven sugars investigated using reactor I and a flow-rate of the make-up of 0.1 ml min^{-1}. With the experimental conditions given above, the detection limits (signal-to-noise ratio 3:1) for the sugars were as follows: D-glucose 55 ng, D-galactose 81 ng, L-arabinose 80 ng, D-xylose 117 ng, D-mannose 0.79 μg, D-xylulose 1.3 μg and D-cellobiose 3.1 μg.

Fig. 7 shows calibration graphs obtained under optimum conditions for D-glucose, D-galactose, L-arabinose, D-mannose and D-xylose using reactor I. As

TABLE III

EFFICIENCIES OF CONVERSION OF SUGARS TO NADH IN REACTOR I WITH THE EXPERIMENTAL PARAMETERS GIVEN IN FIG. 7

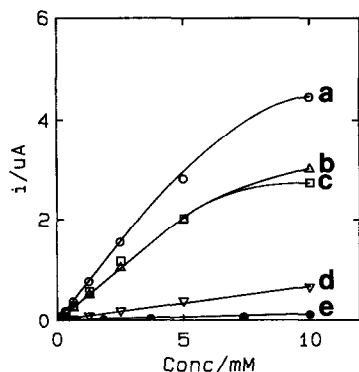| Sugar	Conversion (%)	Sugar	Conversion (%)
L-Arabinose	75	D-Mannose	5.4
D-Cellobiose	0.8	D-Xylose	14
D-Galactose	72	D-Xylulose	3.8
D-Glucose	100		

Fig. 7. Calibration graphs for (a) D-glucose, (b) D-galactose, (c) L-arabinose, (d) D-xylose and (e) D-xylulose with reactor I. Samples were prepared from reference stock solutions. Injection volume, 20 μl; column flow-rates as in Fig. 6.

expected, rectilinear calibration graphs were obtained from the detection limit (signal-to-noise ratio 3:1) at the micromole level over more than two orders of magnitude in concentration, where the concentration of NAD$^+$ in the reactor, 2 mM, becomes the limiting factor[13,15]. This makes quantification of the sugars easy. Diluting spent sulphite liquor 10–100 times prior to injection should give resulting final concentrations of sugars in the sample found within the linear response range of the detection system[2].

Application of the post-column set-up
       A comparison is shown in Fig. 8 between the chromatograms obtained for spent
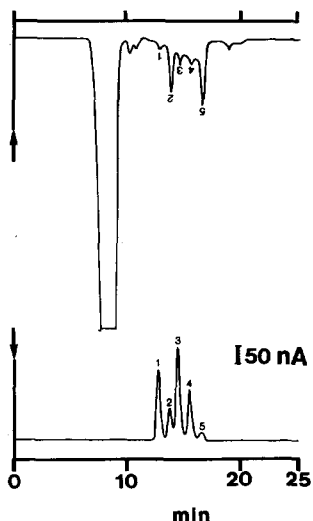

Fig. 8. Chromatograms of 20 μl of spent sulphite liquor, diluted 100-fold, with an RI detector, attenuation 8.0 (upper), and enzyme electrochemical detector (lower). Flow-rate, 0.6 ml min^{-1}; make-up flow, 0.1 ml min^{-1}. Concentrations found: 0.13 mM D-glucose (peak 1), 0.16 mM D-xylose (peak 2), 0.23 mM D-galactose (peak 3), 0.11 mM L-arabinose (peak 4) and 0.51 mM D-mannose (peak 5).

sulphite liquor with the enzymatic electrochemical detector and the generally used refractive index (RI) detector. The post-column detector responds selectively to the five sugars present in the sample whereas the chromatogram obtained with the RI detector shows several unidentified interfering peaks and low sensitivity and selectivity. As is clearly seen, the selectivity of the enzyme electrochemical detection makes quantitative and qualitative analysis of the contents of sugars in the sample very much easier. The main purpose of this study was to work out a sensitive and specific chromatographic system for the determination of sugars in complex biotechnical matrices, where for selectivity reasons in some instances they cannot be monitored using conventional LC detectors such as RI or UV, as shown in Fig. 8.

The inability, however, to separate D-mannose and D-xylulose is a major drawback with the system outlined above. The attempts to increase the resolution through optimization of the metal in the separation column, the injection volume and the flow-rate of the make-up flow did not solve the problem. Peak 5 in Fig. 8 may thus reflect the presence of both D-mannose and D-xylulose in the sample.

Dual-line detection system

D-Mannose is made detectable by the action of immobilized GDH (reaction 1). D-Xylulose, however, is made detectable by the subsequent action of three enzymes, XI, MT and GDH (reactions 6, 5 and 1). By omitting XI from the reactor, D-xylulose should not be detected, as GDH has no activity for D-xylulose.

The combined flow of the effluent and the make-up was therefore split into two detection streams with identical flow-rates by the use of a high-frequency gradient mixer operated in the backward mode. One of the detection streams contained a reactor with co-immobilized MT, GDH and GaDH (reactor III) and the other stream a reactor with co-immobilized XI, MT, GDH and GaDH (reactor II) (Fig. 2). As the flow is split, the resulting flow-rate will be decreased to half its value in each path. A decrease in the flow-rate may result in greater diffusion, yielding a lower resolution. However, by proper optimization of the band-broadening effects, it can be seen in Fig. 9 that this is not so.

Splitting the effluent of the column may also contribute to the band-broadening effects[37]. To minimize this and further reduce the inherent band broadening obtained with post-column reactors, a Zr-treated silica was used as the enzyme carrier in this instance. From an earlier investigation it was found that this Zr–silica has a higher enzyme loading capacity and a higher long-term stability than CPG-10[13]. The higher loading capacity of the Zr–silica should make it possible to make smaller reactors with activity equal of that of a CPG-10 reactor. The small particle size of the Zr–silica should also be advantageous in obtaining better flow characteristics[37]. These two Zr–silica reactors were also high-pressure packed into stainless-steel reactors (see Experimental) to obtain as uniform a packing as possible for optimum flow characteristics.

Fig. 9 shows the two chromatograms obtained for a single injection of spent sulphite liquor spiked with D-cellobiose and D-xylulose. Chromatogram B reflects the selectivity of reactor III containing co-immobilized MT, GDH and GaDH. Here all sugars except D-xylulose are selectively detected. Peak 6 therefore only reflects the concentration of D-mannose. Chromatogram A reflects the selectivity of reactor II containing co-immobilized XI, MT, GDH and GaDH. Peak 6 in this instance is the
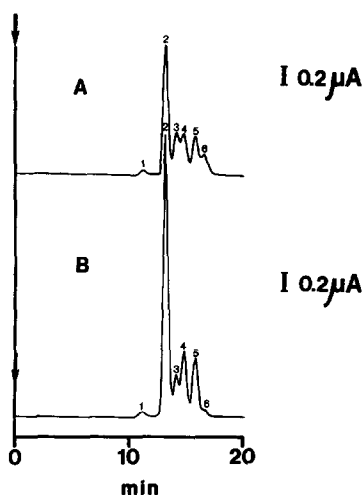
Fig. 9. Dual chromatogram for a single injection (10 μl) of spiked spent sulphite liquor diluted 10-fold, obtained with the parallel detection system of reactors II and III. Flow-rate, 0.6 ml min^{-1}; make-up flow, 0.1 ml min^{-1}; flow-rates through the reactors, 0.35 ml min^{-1}. Concentrations of sugars: 7.5 mM D-cellobiose (peak 1), 4.3 mM D-glucose (peak 2), 7.3 mM D-xylose (peak 3), 2.4 mM D-galactose (peak 4), 2.3 mM L-arabinose (peak 5), 4.5 mM D-mannose (peak 6 in B), 4.5 mM D-mannose and 18 mM D-xylulose (peak 6 in A).

combined response to both D-mannose and D-xylulose. By calibration of the two parallel detection paths simultaneously, the concentration of D-mannose in the sample is obtained from detector B and the concentration of D-xylulose can be calculated by subtracting the response of D-mannose from the total response current of peak 6 obtained from detector A.

TABLE IV

ANALYTICAL DATA FOR SPIKED SPENT SULPHITE LIQUOR, CHROMATOGRAPHED AND DETECTED USING THE PARALLEL DETECTION MODE DEPICTED IN FIG. 2

Reactor	Peak No.[a]	Analyte	R.S.D. (%) (n = 10)
II	1	D-Cellobiose	3.1
	2	D-Glucose	4.0
	3	D-Xylose	5.2
	4	D-Galactose	1.8
	5	L-Arabinose	2.2
	6	D-Xylulose/D-mannose	3.8
III	1	D-Cellobiose	5.1
	2	D-Glucose	1.7
	3	D-Xylose	2.8
	4	D-Galactose	3.7
	5	L-Arabinose	1.8
	6	D-Mannose	3.9

[a] For peak identification, see Fig. 8.

The volume of reactor I is 250 μl whereas that of each of reactors II and III is only 79 μl. Even though a better support was chosen for making reactors II and III, the decrease in reactor volume to only 79 μl has the result that the conversion efficiency for none of the sugars reached 100%. The splitting of the flow after addition of the make-up will also decrease the flow-rate through each of the detection paths compared with the use of only one detection path (reactor I). Therefore, the signal responses to the sugars will decrease and the detection limits will increase compared with the single-line detection system. The repeatability, expressed as relative standard deviation (R.S.D., %), for ten injections of the spiked spent sulphite sample is given in Table IV, and was typically less than 6%.

CONCLUSIONS

The use of a selective post-column detection devise based on immobilized enzymes is clearly demonstrated to be preferred to the generally used RI detector. Spent sulphite liquor constitutes a complex matrix for which an unselective detector is non-optimum. Even if separation problems have not been fully solved, the use of two enzyme-based selective detection systems working in parallel can solve a specific problem. The parallel detection system also greatly reduces the laboratory time and amount of equipment because only a single injection is required with one chromato-graphic system to give a true picture of the composition of the sample.

Reactor I retained 85% of its initial activity after 3–4 weeks. A faster deactivation of the IMERs was observed when the detection system was applied to the determination of sugars in spent sulphite liquor compared with standard solutions prepared in pure water. This may be due to inadequate clean-up of the spent sulphite liquor in which a large number of compounds in the complex matrix may be present which can interact with, inhibit or denature the enzymes. A more elaborate sample clean-up step including a solid-phase extraction procedure is therefore currently being studied in order to overcome this problem and also to make it possible to use this separation and detection system to follow the fermentation of spent sulphite liquor to ethanol described in the Introduction.

REFERENCES

1 K. Skoog and B. Hahn-Hägerdal, *Enzyme Microb. Technol.*, 10 (1988) 66.
2 T. Lindén and B. Hahn-Hägerdal, *Biotechnol. Tech.*, 3 (1989) 189.
3 F. Tjerneld, I. Persson, P.-Å. Albertsson and B. Hahn-Hägerdal, *Biotechnol. Bioeng. Symp.*, No. 15 (1985) 419.
4 B. Hahn-Hägerdal, S. Berner and K. Skoog, *Appl. Microbiol. Biotechnol.*, 24 (1986) 287.
5 T. Lindén and B. Hahn-Hägerdal, *Enzyme Microb. Technol.*, 11 (1989) 583.
6 E. Dominguez, B. Hahn-Hägerdal, G. Marko-Varga and L. Gorton, *Anal. Chim. Acta*, 213 (1988) 139.
7 G. Marko-Varga, E. Dominguez, L. Gorton and B. Hahn-Hägerdal, *Anal. Chim. Acta*, 225 (1989) 263.
8 R. W. Murray, A. G. Ewing and R. A. Durst, *Anal. Chem.*, 59 (1987) 379A.
9 S. Dong and Y. Wang, *Electroanalysis*, 1 (1989) 99.
10 L. Gorton, *J. Chem. Soc., Faraday Trans. I*, 82 (1986) 1245.
11 L. Gorton, B. Persson, M. Polasek and G. Johansson, *Proceedings of ElectroFinnAnalysis, 1988*, Plenum Press, New York, in press.
12 G. Marko-Varga, *J. Chromatogr.*, 408 (1987) 157.
13 G. Marko-Varga, *Anal. Chem.*, 61 (1989) 831.
14 E. Hoffmann, G. Marko-Varga, I. Csiky and J. Å. Jönsson, *Int. J. Environ. Anal. Chem.*, 25 (1986) 161.
15 R. Appelqvist, G. Marko-Varga, L. Gorton, A. Torstensson and G. Johansson, *Anal. Chim. Acta*, 169 (1985) 237.
16 H. H. Weetal and R. A. Messing, in M. L. Hair (Editor), *The Chemistry of Biosurfaces*, Vol. II, Marcel Dekker, New York, 1972, Ch. 12.
17 G. Johansson, L. Ögren and B. Olsson, *Anal. Chim. Acta*, 145 (1983) 71.
18 T. E. Barman, *Enzyme Handbook*, Vol. I, Springer, Heidelberg, 1969, p. 72.
19 R. Vormbrock, in H. U. Bergmeyer (Editor), *Methods of Enzymatic Analysis*, Vol. 6, Verlag Chemie, Weinheim, 3rd ed., 1984, p. 172.
20 B. J. van Schie, R. J. Rouwenhorst, J. A. M. De Bont, J. P. van Dijken and J. G. Kueven, *Appl. Microbiol. Biotechnol.*, 26 (1987) 560.
21 W.-P. Chen, *Process Biochem.*, June/July (1980) 30.
22 W.-P. Chen, *Process Biochem.*, August/September (1980) 36.
23 K. J. Schray and I. A. Rose, *Biochemistry*, 10 (1971) 1058.
24 J. M. Young, K. J. Schray and A. S. Mildvan, *J. Biol. Chem.*, 250 (1975) 9021.
25 H. Kersters-Hilderson, M. Claeyssens, C. Van Doorslaer and C. K. De Brutne, *Carbohydr. Res.*, 47 (1976) 269.
26 Z. Samec and P. J. Elving, *J. Electroanal. Chem.*, 144 (1983) 217.
27 J. Moiroux and P. J. Elving, *J. Am. Chem. Soc.*, 103 (1980) 6533.
28 A. Schelter-Graf, H.-L. Schmidt and H. Huck, *Anal. Chim. Acta*, 163 (1984) 299.
29 S. P. J. Brooks and C. H. Suelter, *Anal. Biochem.*, 176 (1989) 1.
30 B. Mattiasson, in T. N. S. Chang (Editor), *Biomedical Applications of Immobilized Enzymes and Proteins*, Vol. 2, Plenum Press, New York, 1977, p. 261.
31 E. Dominguez, G. Marko-Varga, B. Hahn-Hägerdal and L. Gorton, in preparation.
32 G. Marko-Varga, Lund, unpublished results, 1987.
33 P. Jonsson and O. Samuelsson, *Anal. Chem.*, 39 (1967) 1156.
34 S. J. Angyal, *Pure Appl. Chem.*, 35 (1973) 131.
35 R. W. Goulding, *J. Chromatogr.*, 103 (1975) 229.
36 P. Vrátny, U. A. Th. Brinkman and R. W. Frei, *Anal. Chem.*, 57 (1985) 224.
37 I. S. Krull (Editor), *Reaction Detection in Liquid Chromatography*, Marcel Dekker, New York, 1986.